ground state; the $S = {}^3/_2$ state would be an excited state in contradiction with the ground-state assignment of the above signal. An $S = {}^3/_2$ signal could conceivably arise from a high-spin Ni(III) ($S = {}^3/_2$) with weak or vanishing coupling to an EPR-silent Ni(II) ($S = 1$); however, this appears unlikely, given that all known Ni(III) complexes to date are low spin[18] and that in all complexes of BPMP involving two paramagnetic metal ions thus far some degree of coupling is observed.[1a,b,d-f]

The observed ferromagnetic coupling may be rationalized by an examination of the magnetic orbitals of the two nickel centers under the assumption that the phenolate bridge dominates the coupling interaction of the complex, an assumption supported by our studies of FeCuBPMP complexes.[1d,e] Jahn-Teller elongation of the low-spin Ni(III) (d^7) site along an axis orthogonal to the phenolate bond[19,20] would place the magnetic orbital (d_{z^2})[21] parallel to the elongation axis and orthogonal to the phenolate bond, engendering ferromagnetic coupling. A Jahn-Teller elongation has previously been observed in the crystal structure of $[Fe^{III}Cu^{II}BPMP(O_2CCH_3)_2](BPh_4)_2$,[1d] in which case, the magnetic orbital ($d_{x^2-y^2}$) is directed along the phenolate bond and antiferromagnetic coupling is observed. It is not unreasonable to propose similar structural properties in the $Ni^{III}Ni^{II}$ complex, which would explain the observed spectroscopic result.

In conclusion, we have reported the unambiguous observation of an integer-spin EPR signal from an antiferromagnetically coupled $Ni^{II}Ni^{II}$ cluster. The existence of such a signal may help in the further investigations of similar centers in model inorganic complexes as well as in the active site of urease. In addition, we have generated and characterized some properties of the first $Ni^{III}Ni^{II}$ mixed-valence complex.

Acknowledgment. We are grateful to Prof. J. D. Lipscomb for use of his EPR spectrometer. This work was supported by National Institutes of Health Grant GM38767 (L.Q.), Postdoctoral Fellowship GM12996 (M.P.H.), and Predoctoral Traineeship GM08277 (T.R.H.).

(18) (a) Lappin, A. G.; Murray, C. K.; Margerum, D. W. *Inorg. Chem.* **1978**, *17*, 1630-1634. (b) Haines, R. I.; McAuley, A. *Coord. Chem. Rev.* **1981**, *39*, 77-119. (c) Salerno, J. C. In *The Bioinorganic Chemistry of Nickel*; Lancaster, J. R., Ed.; VCH: New York, 1988; pp 53-72.
(19) Lovecchio, F. V.; Gore, E. S.; Busch, D. H. *J. Am. Chem. Soc.* **1974**, *96*, 3109-3118.
(20) de Castro, B.; Freire, C. *Inorg. Chem.* **1990**, *29*, 5113-5119.
(21) The EPR spectra of low-spin Ni(III) complexes associate the magnetic orbital with the d_{z^2} orbital.[18]

Department of Chemistry
University of Minnesota
Minneapolis, Minnesota 55455

Theodore R. Holman
Michael P. Hendrich
Lawrence Que, Jr.*

Received July 26, 1991

Characterization of Fe(OEP) π-Cation Radicals

We report the characterization of two classes of π-cation-radical derivatives of (octaethylporphinato)iron(III): $[Fe(OEP^{\bullet})(OClO_3)_2]$,[1] and $[Fe(OEP^{\bullet})(Cl)]Y$, where $Y = ClO_4^-$ or $SbCl_6^-$. A combination of crystal structure determination, magnetic susceptibility measurement, and Mössbauer spectroscopy leads to an unambiguous assignment of the iron spin states and gives insight into the nature of the porphyrin radical/iron spin coupling. Our conclusions are distinctly different from those recently reported by Nakashima et al.,[2,3] which were based solely on magnetic susceptibility results.

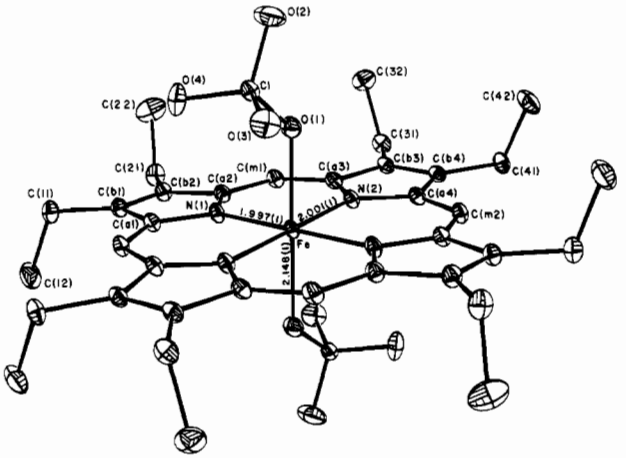

Figure 1. ORTEP diagram of the molecular structure of the $[Fe(OEP^{\bullet})(OClO_3)_2]$ complex. Thermal ellipsoids are drawn at the 50% probability level. Hydrogen atoms omitted for clarity.

Six-coordinate $[Fe(OEP^{\bullet})(OClO_3)_2]$ was prepared by oxidation of $[Fe(OEP)(OClO_3)]$ with thianthrenium perchlorate.[4-8] The single-crystal sample, prepared from [Fe(OEP)Cl], has a minor chloride impurity; bulk samples are homogeneous by Mössbauer criteria. The molecular structure of $[Fe(OEP^{\bullet})(OClO_3)_2]$ is illustrated in Figure 1.[9] The monomeric complex has two axial perchlorate ligands with an in-plane iron atom located at an inversion center. The average value of the Fe-N_p bond distances is 1.999 (2) Å, which is inconsistent with a high-spin state for iron.[11] The analogous $TTP^{\bullet}$ complex[6] has an average Fe-N_p bond distance of 2.068 (21) Å, consistent with the assigned high-spin state. The porphinato core is planar, consistent with the required inversion symmetry. Both this molecular structure and the diagnostically large quadrupole splitting in the zero-field Mössbauer spectrum ($\Delta E_q = 3.00$ mm/s and $\delta = 0.43$ mm/s, 4.2 K) show that the iron(III) atom has an *admixed intermediate-spin* state, rather than the high-spin state assumed by others[2] and seen for the analogous $TPP^{\bullet}$ and $TTP^{\bullet}$ derivatives.[6,12] The intermedi-

(1) Abbreviations: OEP, TPP, and TTP, dianions of octaethyl-, tetraphenyl-, and tetratolylporphyrin, respectively; π-cation-radical derivatives are indicated with a raised dot in the formula (i.e., $OEP^{\bullet}$).

(2) Nakashima, S.; Ohya-Nishiguchi, H.; Hirota, N.; Fujii, H.; Morishima, I. *Inorg. Chem.* **1990**, *29*, 5207.
(3) Our high-temperature magnetic moments for $[Fe(OEP^{\bullet})(OClO_3)_2]$ are significantly lower than those of Nakashima et al. Although our magnetic susceptibility data for $[Fe(OEP^{\bullet})(Cl)][SbCl_6]$ are quite similar to those of Nakashima et al., we are unable to achieve satisfactory fits with their parameters.
(4) Gans, P.; Marchon, J.-C.; Reed, C. A.; Regnard, J.-R. *Nouv. J. Chim.* **1981**, *5*, 203.
(5) Murata, Y.; Shine, H. J. *J. Org. Chem.* **1969**, *34*, 3368.
(6) Gans, P.; Buisson, G.; Duée, E.; Marchon, J.-C.; Erler, B. S.; Scholz, W. F.; Reed, C. A. *J. Am. Chem. Soc.* **1986**, *108*, 1223.
(7) Shimomura, E. T.; Phillippi, M. A.; Goff, H. M.; Scholz, W. F.; Reed, C. A. *J. Am. Chem. Soc.* **1981**, *103*, 6778. Phillippi, M. A.; Goff, H. M. *J. Am. Chem. Soc.* **1982**, *104*, 6778.
(8) Synthetic details for single crystals and bulk samples of $[Fe(OEP^{\bullet})(OClO_3)_2]$ are given in the supplementary material. UV-vis (CH_2Cl_2 solution): λ_{max} 378 (Soret), 480 nm. IR (KBr) $\nu(OEP^{\bullet})$ 1531 cm^{-1} (broad); $\nu(ClO_4)$ 1145 (strong), 1108 (strong, broad), 636, 627 cm^{-1}.
(9) $[Fe(OEP^{\bullet})(OClO_3)_2]$ crystallizes in the triclinic space group $P\bar{1}$, a = 9.530 (3) Å, b = 9.580 (2) Å, c = 10.756 (2) Å, α = 88.96 (2)°, β = 77.06 (2)°, γ = 68.72 (2)°, V = 889.7 Å^3, and $Z = 1$. A total of 8092 reflections were measured (6082 unique) at 123 K and 5184 reflections having $(\sin\theta)/\lambda < 0.742$ and $F_o \geq 3.0\sigma(F_o)$ were taken as observed. The structure was solved using the program DIRDIF[10] and difference Fouriers. A small amount of an impurity (<7% of [Fe(OEP)(Cl)]) was included in the final model. Unlike the bulk samples, single crystals were derived from [Fe(OEP)(Cl)] rather than $[Fe(OEP)(OClO_3)]$. Least-squares refinement of the model based on 298 variables with anisotropic thermal parameters for all major occupancy non-hydrogen atoms and fixed, idealized hydrogen atoms leads to $R_1 = 0.041$, $R_2 = 0.054$, and goodness of fit = 1.91.
(10) Beurskens, P. T.; Bosman, W. P.; Doesbury, H. M.; Gould, R. O.; van den Hark, Th. E. M.; Prick, P. A.; Noordik, J. H.; Stempel, M.; Smits, J. M. M. *DIRDIF*; Technical Report 1984/1; Crystallography Laboratory: Toernooiveld, 6525 Ed Nijmegen, The Netherlands.
(11) Scheidt, W. R.; Reed, C. A. *Chem. Rev.* **1981**, *81*, 543.

0020-1669/92/1331-0939$03.00/0

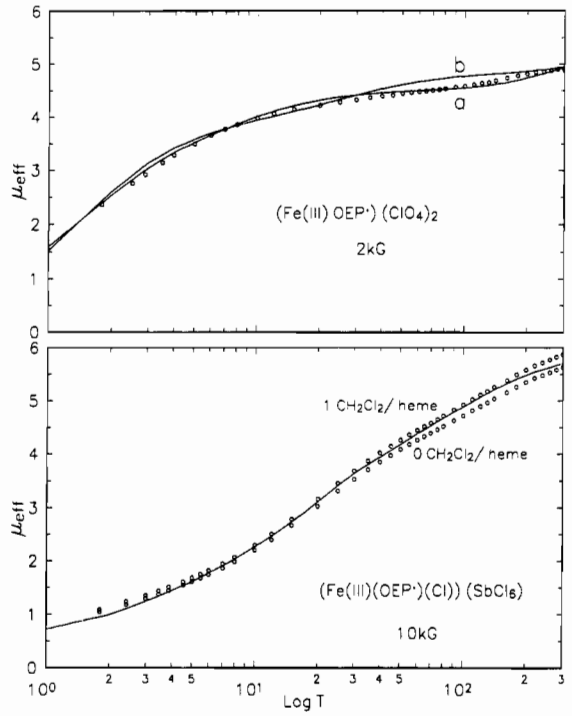

Figure 2. (A) Magnetic susceptibility data for $[Fe(OEP^{\bullet})(OClO_3)_2]$ showing the agreement between the observed and calculated values. Solid lines are simulations based on models (a and b) as described in the text. (B) Magnetic susceptibility data for $[Fe(OEP^{\bullet})(Cl)]_2(SbCl_6)_2$ showing the agreement between the observed (circles) and calculated (lines) values using the two coupling schemes described in the text, which give virtually identical fits. The calculated magnetic moment values shown are based on both one and zero molecules of solvation; the solvent content of microcrystalline $[Fe(OEP^{\bullet})(Cl)]_2(SbCl_6)_2$ is thought to be intermediate to these limits.

ate-spin state must result from the increased tetragonality in the octaethylporphyrin complex that arises from the increased in-plane σ-donation of H_2OEP relative to H_2TPP and H_2TTP derivatives. Clearly, this admixed intermediate-spin state must be the starting point for any detailed fit of the temperature-dependent magnetic susceptibility data.[13] Thus both a description of the admixed intermediate-spin iron(III) state and how it is coupled to the radical spin are required for a quantitative description of the magnetic properties of the complex. To date, we have found two different Maltempo[14] mixed-spin models that lead to acceptable fits of the susceptibility *and* the magnetic Mössbauer data. The first model (a) has a spin–orbit coupling of 139 cm^{-1}, a $^6A_1$ state 278 cm^{-1} above the $S = {}^3/_2$ quartet (a 16% admixture of $S = {}^5/_2$ in the $S = {}^3/_2$ iron(III) multiplet[15]) and the iron(III) spin system weakly antiferromagnetically coupled to the radical spin ($-2J = -1.91$ cm^{-1}). The second, more complex, model (b) has a spin–orbit coupling of 417 cm^{-1}, a $^6A_1$ state 348 cm^{-1} above the $S = {}^3/_2$ quartet (an ~30% admixture of $S = {}^5/_2$ in the $S = {}^3/_2$ iron(III) multiplet) and the iron(III) spin antiferromagnetically coupled ($-2J = -30$ cm^{-1}) to the quartet but ferromagnetically coupled ($-2J = 42$ cm^{-1}) to the sextet component. The first model gives better susceptibility data fits as shown in Figure 2A while the second gives better fits to the temperature dependence of the magnetic splitting of the Mössbauer spectra (Figure S2). Both

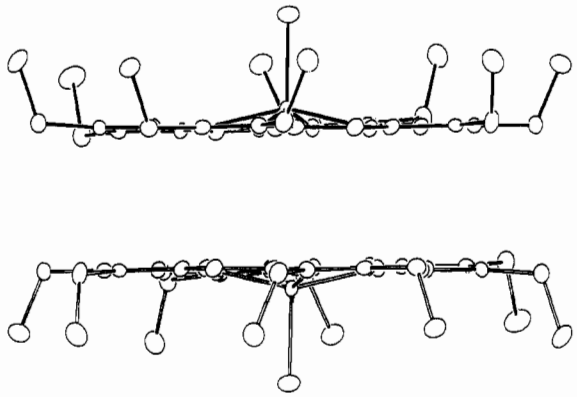

Figure 3. ORTEP drawing of the $[Fe(OEP^{\bullet})(Cl)]_2^{2+}$ dimer. Thermal ellipsoids are drawn at the 50% probability level. The horizontal axis is parallel to and the vertical axis is normal to the best plane of the 24-atom porphyrin core; the perpendicular mean plane separation is 3.24 Å.

models predict that an EPR signal for this "even electron" system might be observed; a broad EPR signal is seen between 0.5 and 6.0 kG at temperatures above 20 K.[16] The characterization of related six-coordinate $[Fe(OEP^{\bullet})(Y)_2]$ species, currently in progress, is expected to clarify the coupling model.

$[Fe(OEP^{\bullet})(Cl)]^+$ salts were prepared by oxidation of [Fe(OEP)(Cl)] with thianthrenium perchlorate or tris(*p*-bromophenyl)aminium hexachloroantimonate $[(BrC_6H_4)_3NSbCl_6]$.[17] Bulk samples of the perchlorate salt were always found to be contaminated with $[Fe(OEP^{\bullet})(OClO_3)_2]$ while the hexachloroantimonate salt can be obtained pure by Mössbauer criteria. Single crystals of the perchlorate salt were obtained. The coordination geometry around the iron(III) atom suggests a ***high-spin*** state: Fe–Cl = 2.186 (1) Å, Fe–N_p = 2.058 (5) Å, with the iron atom displaced 0.43 Å out of plane. Crystalline $[Fe(OEP^{\bullet})(Cl)]ClO_4$ exists as a tight cofacial π–π dimer with an interplanar separation of 3.24 Å. Orthogonal views of the solid-state dimer are given in Figures 3 and S3. Interestingly, the essentially planar inner 16-membered porphyrin ring shows the same alternating bond distance pattern first noted in dimeric, diamagnetic $[Zn(OEP^{\bullet})(H_2O)]_2(ClO_4)_2$,[20] and is presumably the result of the strong coupling (pairing) of the $S = {}^1/_2$ radical spins on the two porphyrin rings. The values of these bond distances are shown in Figure S4.

Consistent with this crystal structure, the zero-field Mössbauer spectrum of $[Fe(OEP^{\bullet})(Cl)]ClO_4$ ($\Delta E_q = 0.59$, $\delta = 0.41$ mm/s at 4.2 K) and of $[Fe(OEP^{\bullet})(Cl)][SbCl_6]$ ($\Delta E_q = 0.71$, $\delta = 0.42$ mm/s at 4.2 K) clearly indicate that the iron(III) atom is high spin. Nevertheless, nominally five-coordinate $[Fe(OEP^{\bullet})(Cl)]ClO_4$ differs from its analogous $TTP^{\bullet}$ derivative in the degree of intermolecular interaction. This probably has a substantial influence on the coupling between the various unpaired electrons of the system and must be considered in the development of quantitative fits to the magnetic data. Thus, inter-ring radical coupling, clearly shown to be important in the diamagnetic dimer $[Zn(OEP^{\bullet})(H_2O)]_2(ClO_4)_2$,[20] and coupling between the radical and

(12) Goff, on the basis of NMR proton shift values, suggests that the $[Fe(TPP^{\bullet})(OClO_3)_2]$ has substantial spin-admixed character for iron(III) in *solution*: Boersma, A. D.; Goff, H. *Inorg. Chem.* **1984**, *23*, 1671.
(13) Magnetic susceptibility measurements were performed on ground, compressed samples (~30 mg) in aluminum buckets on a SHE Model 905 SQUID susceptometer at 2 and 10 kG over the temperature range 2–300 K.
(14) Maltempo, M. M.; Moss, T. H. *Q. Rev. Biophys.* **1976**, *9*, 181.
(15) It is to be noted that the percentage of the $S = {}^5/_2$ state in the admixture is extremely sensitive to the value of the high-temperature magnetic moment and shows significant variation within the range of probable experimental errors of the susceptibility values.
(16) This EPR signal increases in intensity with temperature, indicating that it is due to an excited state in the coupled iron(III)–porphyrin radical system.
(17) Complete synthetic details are in the supplementary material. Some spectroscopic data has been reported previously: see refs 6 and 7.
(18) The complex crystallizes in the monoclinic space group $C2/c$, with a = 27.454 (7) Å, b = 15.322 (3) Å, c = 19.802 (3) Å, β = 116.14 (2)°, V = 7477.4 Å^3, and Z = 8. A total of 11 146 reflections (9178 unique) were measured at 123 K, and 5787 reflections having $(\sin\theta)/\lambda < 0.669$ and $F_o \geq 3.0\sigma(F_o)$ were taken as observed. The structure was solved using the Patterson interpretation and tangent refinement routines of SHELXS.[19] Least-squares refinement of the model based on 541 variables with anisotropic thermal parameters for all nonhydrogen atoms and fixed, idealized hydrogen atoms leads to $R_1 = 0.069$, $R_2 = 0.063$, and goodness of fit = 1.45.
(19) Sheldrick, G. *SHELXS*; Institut für Anorganische Chemie der Universitat: Göttingen, Germany, 1986.
(20) Song, H.; Orosz, R. D.; Reed, C. A.; Scheidt, W. R. *Inorg. Chem.* **1990**, *29*, 4274.

its associated $S = {}^5/_2$ iron atom, as well as zero-field splitting for iron, could all be important. Given this number of variables, a unique fit to the data cannot be assured. Our current best models have (i) strong coupling between the two radical spins ($-2J = -70$ cm^{-1}), slightly weaker coupling between each $S = {}^5/_2$ Fe(III) center and its associated radical ($-2J' = -63$ cm^{-1}), and a zero-field splitting constant of 35 cm^{-1} or (ii) strong coupling between high-spin iron and porphyrin radical ($-2J\vec{S}\cdot\vec{s}$, with $-2J = -49$ cm^{-1}, $D = 21$ cm^{-1}) and weak coupling of the total spins between the dimer units $-2J'(\vec{S} + \vec{s})\cdot(\vec{S}' + \vec{s}')$ with $-2J' = -3.5$ cm^{-1} (antiferromagnetic).[21] This latter model is similar to that used by Lang et al.[22] for a fit of the magnetic susceptibility data of [Fe(TPP•)(Cl)][$SbCl_6$]. Both models give an excellent fit to the susceptibility data over the entire temperature range as shown in Figure 2B. Detailed Mössbauer investigations are underway but are complicated by intermediate relaxation rate effects from 4 K up to 100 K. Magnetic ordering below 2 K in a 6-T applied field also occurs.

In summary, characterization of π-cation-radical derivatives of (octaethylporphinato)iron(III), [Fe(OEP•)($OClO_3$)$_2$], and [Fe(OEP•)(Cl)]Y, Y = ClO_4^- or $SbCl_6^-$, shows that the spin-state assignment and spin-coupling mechanisms are more complex than those of the analogous TPP• species and more complex than those assumed by Nakashima et al.[2,3] An admixed intermediate-spin state for iron in a π-cation-radical derivative has been demonstrated for the first time. The question of the magnitude of the coupling between metal spins with a_{1u} radicals (OEP•) compared to a_{2u} radicals (TPP•) remains open.

Acknowledgment. We acknowledge, with thanks, the support of the National Institutes of Health under Grants GM-38401 (W.R.S.), GM-23851 (C.A.R.), and GM-16406 (P.G.D.).

Supplementary Material Available: Tables SIII–SV, giving atomic coordinates, bond distances, and bond angles for [Fe(OEP•)($OClO_3$)$_2$], Tables SVI–SVIII, giving atomic coordinates, bond distances, and bond angles for [Fe(OEP•)(Cl)]ClO_4, Figure S1, showing a formal diagram of the core of [Fe(OEP•)($OClO_3$)$_2$], Figure S2, containing diagrams showing the temperature-dependent fits of the magnetic Mössbauer spectral data for [Fe(OEP•)($OClO_3$)$_2$], Figure S3, showing an ORTEP drawing of the [Fe(OEP•)(Cl)]$_2^{2+}$ dimer viewed down the Fe···Fe axis, Figure S4, showing the alternant bond distances in the inner 16-membered rings of [Fe(OEP•)(Cl)]$_2^{2+}$, and text giving the complete synthetic details (14 pages); Tables SI and SII, listing calculated and observed structure factors (×10) (31 pages). Ordering information is given on any current masthead page.

(21) The $^5/_2$ iron spin system is represented by $\vec{S}$ and the radical spin system by $\vec{s}$.

(22) Lang, G.; Boso, B.; Erler, B. S.; Reed, C. A. *J. Chem. Phys.* **1986**, *84*, 2998.

(23) Work also performed at the Department of Physics, University of Illinois.

Department of Chemistry and Biochemistry, University of Notre Dame, Notre Dame, Indiana 46556 — **W. Robert Scheidt***, **Hungsun Song**, **Kenneth J. Haller**, **Martin K. Safo**

Department of Chemistry, University of Southern California, Los Angeles, California 90089-0744 — **Robert D. Orosz**, **Christopher A. Reed***

Department of Physics, University of Illinois, Urbana, Illinois 61801 — **Peter G. Debrunner***

Department of Physics, Knox College, Galesburg, Illinois 61401 — **Charles E. Schulz*,23**

Received October 17, 1991

Articles

Contribution from the Institut für Anorganische und Analytische Chemie and the Institut für Organische Chemie, Technische Universität Berlin, Strasse des 17. Juni 135, D-1000 Berlin 12, Germany

Generation and Characterization of Dihydroxy Disulfide, HOSSOH: The Chainlike Isomer of Thiosulfurous Acid[1]

Heinar Schmidt,[2a] Ralf Steudel,*[,2a] Detlev Sülzle,[2b] and Helmut Schwarz[2b]

Received August 26, 1991

Dissociative ionization of diisopropoxy disulfide ($C_3H_7OSSOC_3H_7$) by 70-eV electron impact gives rise to $H_2S_2O_2^{\bullet+}$ ions, whose collisional activation (CA) mass spectrum is in keeping with the connectivity of HOSSOH$^{\bullet+}$. This ion has been successfully neutralized and reionized in a two-stage collision experiment. This neutralization–reionization (NR) mass spectrum confirms previous theoretical predictions that HOSSOH resides in a potential minimum deep enough to prevent the species from isomerization–dissociation processes during the experiment (about 10^{-5} s). The experimental assignments are supported by the study of HOSSOD$^{\bullet+}$ and DOSSOD$^{\bullet+}$ generated accordingly by electron-impact-induced loss of propene from $C_3H_7OSSOC_3D_7$ and $C_3D_7OSSOC_3D_7$, respectively.

Introduction

Thiosulfurous acid is unstable in condensed phases, as it is common for all lower oxyacids of sulfur.[3] The free acid, $H_2S_2O_2$, or its anion is regarded to be the primary product in the reaction between sulfur dioxide and hydrogen sulfide,[4] well-known from the aqueous Wackenroder reaction and the industrially important Claus process, eq 1.

$$H_2S + SO_2 \rightarrow H_2S_2O_2 \quad (1)$$

(1) Sulfur Compounds. 148. Part 147: Miaskiewicz, K.; Steudel, R. *Angew. Chem.* **1992**, *104*, 87–89; *Angew. Chem., Int. Ed. Engl.* **1992**, *31*, 58–59.

(2) (a) Institut für Anorganische und Analytische Chemie. (b) Institut für Organische Chemie.

(3) (a) Greenwood, N. N.; Earnshaw, A. *Chemistry of the Elements*; Pergamon Press: Oxford, U.K., 1984; p 834. (b) Holleman-Wiberg; *Lehrbuch der Anorganischen Chemie*; W. de Gruyter: Berlin, 1985; p 501. (c) Lyons, D.; Nickless, G. In *Inorganic Sulphur Chemistry*; Nickless, G., Ed.; Elsevier: Amsterdam, 1968; Chapter 14, p 509.

(4) (a) Stamm, H.; Goehring, M. *Z. Anorg. Allg. Chem.* **1939**, *242*, 413. (b) Schenk, P. W.; Steudel, R. *Angew. Chem.* **1965**, *77*, 437; *Angew. Chem., Int. Ed. Engl.* **1965**, *4*, 402. (c) *Gmelin Handbuch der Anorganischen Chemie*; Springer Verlag: Berlin, 1980; Schwefel, Ergänzungsband 3, p 195. (d) Ab-initio calculations on H_2S, SO_2, and $(SOH)_2$ at the HF/6-31G* level indicate that reaction 1 is exothermic by 13 kJ/mol: Miaskiewicz, K.; Steudel, R. Unpublished results, 1991.

0020-1669/92/1331-0941$03.00/0